

Periodicities in Solar Coronal Mass Ejections

Yu-Qing Lou^{1,2,3}, Yu-Ming Wang^{1,4}, Zuhui Fan^{1,5}, Shui Wang^{1,4}, JingXiu Wang^{1,5}

¹*National Astronomical Observatories, Chinese Academy of Sciences, A20, Datun Road, Beijing, 100012 China*

²*Physics Department, Tsinghua Center for Astrophysics, Tsinghua University, Beijing 100084, China*

³*Department of Astronomy and Astrophysics, The University of Chicago, Chicago, Illinois 60637 USA; lou@oddjob.uchicago.edu*

⁴*University of Science and Technology of China, Hefei, Anhui, 230026, China*

⁵*Beijing Astrophysical Center and Department of Astronomy, CAS-PKU, Peking University, Beijing 100871 China.*

Accepted Received; in original form ...

ABSTRACT

Mid-term quasi-periodicities in solar coronal mass ejections (CMEs) during the most recent solar maximum cycle 23 are reported here for the first time using the four-year data (February 5, 1999 to February 10, 2003) of the *Large Angle Spectrometric Coronagraph (LASCO)* onboard the *Solar and Heliospheric Observatory (SOHO)*. In parallel, mid-term quasi-periodicities in solar X-ray flares (class $>M5.0$) from the *Geosynchronous Operational Environment Satellites (GOES)* and in daily averages of Ap index for geomagnetic disturbances from the *World Data Center (WDC)* at the *International Association for Geomagnetism and Aeronomy (IAGA)* are also examined for the same four-year time span. By Fourier power spectral analyses, the CME data appears to contain significant power peaks at periods of $\sim 358 \pm 38$, $\sim 272 \pm 26$, $\sim 196 \pm 13$ days and so forth, while except for the $\sim 259 \pm 24$ -day period, X-ray solar flares of class $\gtrsim M5.0$ show the familiar Rieger-type quasi-periods at $\sim 157 \pm 11$, $\sim 122 \pm 5$, $\sim 98 \pm 3$ days and shorter ones until $\sim 34 \pm 0.5$ days. In the data of daily averages of Ap index, the two significant peaks at periods $\sim 273 \pm 26$ and $\sim 187 \pm 12$ days (the latter is most prominent) could imply that CMEs (periods at $\sim 272 \pm 26$ and $\sim 196 \pm 13$ days) may be proportionally correlated with quasi-periodic geomagnetic storm disturbances; at the speculative level, the $\sim 138 \pm 6$ -day period might imply that X-ray flares of class $\gtrsim M5.0$ (period at $\sim 157 \pm 11$ days) may drive certain types of geomagnetic disturbances; and the $\sim 28 \pm 0.2$ -day periodicity is most likely caused by recurrent high-speed solar winds at the Earth's magnetosphere. For the same three data sets, we further perform Morlet wavelet analysis to derive period-time contours and identify wavelet power peaks and timescales at the 99 percent confidence level for comparisons. Several conceptual aspects of possible equatorially trapped Rossby-type waves at and beneath the solar photosphere are discussed.

Key words: oscillations — space weather — Sun: activities — corona — coronal mass ejections — magnetic fields

1 INTRODUCTION

Mid-term quasi-periodicities (one to several months or longer) in various diagnostics of solar flare activities and sunspot numbers or areas etc. during a few years around the solar maximum phase have been extensively searched for and monitored at many electromagnetic wavelengths (Rieger et al. 1984; Kiplinger et al. 1984; Dennis 1985; Ichimoto et al. 1985; Delache et al. 1985; Bogart & Bai 1985; Bai & Sturrock 1987; Oliver et al. 1988; Ribes et al. 1987; Lean & Brueckner 1989; Özgür & Ataç 1989; Lean 1990; Carbonell & Ballester 1990; Dröge et al. 1990; Pap et al. 1990; Kile & Cliver 1991; Verma et al. 1992; Ballester et al. 1999; Cane, Richardson, & von Rosenvinge 1998). These activities of observational re-

search were triggered by the landmark discovery by Rieger et al. (1984) of a ~ 154 -day quasi-period in solar γ -ray flare rates registered by the *Gamma-Ray Spectrometer (GRS)* onboard the *Solar Maximum Mission (SMM)* two decades ago. Besides this oft-quoted quasi-period of ~ 150 -160 days, there are other notable quasi-periods around ~ 128 , ~ 102 , ~ 78 , and ~ 51 days during the maxima of different solar cycles (Dennis 1985; Bai 1992; Bai & Sturrock 1991) from various data sets. Empirically, these quasi-periods seem to hint at quasi-subharmonics of equatorial solar rotation period (e.g., Sturrock & Bai 1992; Bai & Sturrock 1993).

As to the plausible physical origin of such quasi-subharmonics with periods *longer* than the solar rotation period, we proposed recently (Lou 2000a, b) that, in the

statistical sense, the existence of equatorially trapped large-scale (scales comparable to R_{\odot}) Rossby-type waves (Rossby et al. 1939; Papaloizou & Pringle 1978; Provost et al. 1981; Saio 1982; Wolff & Blizard 1986; Wolff 1998) may be ultimately responsible for quasi-periodically modulating or triggering smaller-scale magnetic catastrophes in solar active regions. In this scenario, solar magnetic active regions become, recurrently, vulnerable to catastrophes via statistical accumulations of magnetic stresses and energies through magneto-convective turbulence.

In terms of specific observational diagnostics, we suggested (Lou 2000b) that the photospheric magnetic flux emergence might be triggered via magnetohydrodynamic (MHD) buoyance instabilities (Parker 1955) modulated by equatorially trapped Rossby-type waves owing to the presence of large-scale subphotospheric magnetic flux (Gilman 1969; Lou 1987; see Ballester et al. 2002 for most recent emerging magnetic flux observations), that large-scale coherent velocity patterns or “cells” may exist over the solar surface (see Beck, Duvall, & Scherrer 1998 and Ulrich 2001), and that more precise measurements of solar surface elevation may reveal $\lesssim 0.1''$ variations (see Kuhn et al. 2000 for much smaller 100-m high “hills” with an azimuthal separation of $[8.7 \pm 0.6] \times 10^4 \text{ km}$). As Rossby-type waves involve fairly slow and large-scale vortical oscillatory disturbances with periods longer than the solar rotation period, we speculated (Lou 2000a, b) that an uninterrupted time sequence of large-scale coronal mass ejection (CME) events might contain similar mid-term quasi-periodicities. The *LASCO/SOHO* global observations of solar CMEs in space offer an unprecedented and unique opportunity for such an investigation. Uninterrupted *LASCO/SOHO* CME data is now available for four years (February 5, 1999 to February 10, 2003).

Meanwhile, we examine possible mid-term quasi-periodicities for powerful X-ray solar flares of class $>M5.0$ and daily averages of Ap index for geomagnetic storm disturbances for several reasons. First, as a proxy of γ -ray flares (Rieger et al. 1984), strong X-ray flares are known to contain Rieger-type periodicities during past solar maxima. We would like to reconfirm this feature and provide a test of our current data analysis at the same time. Secondly, strong X-ray flares might correlate with global CMEs in some statistical sense. Thirdly, in terms of both space weather and solar terrestrial interactions, we would like to establish possible correlations among CMEs, intense X-ray flares, and geomagnetic disturbances characterized by daily averages of Ap index. Systematic investigations on quasi-periodicities may reveal such correlations in a unique manner.

For all three data sets, we shall first use Fourier analysis to identify possible quasi-periodicities. To complement the Fourier spectra, we further carry out Morlet wavelet analyses to derive contour plots in period-time domains for the same three time series of CME, X-ray solar flares, and geomagnetic Ap index data, respectively. With a few exceptions, major peaks identified in the wavelet analyses are roughly consistent with major peaks in the Fourier power spectral analyses. Additional information of when certain quasi-periodicities occur or recur in different data sets may provide valuable clues for possible physical connections.

In broader astrophysical contexts, we note in passing that global MHD tidal waves including Alfvén-Rossby type

Figure 1. (a) Daily counts of CME events from LASCO for the four-year time span shown on top. (b) Fourier power spectrum of the CME data. (c) Comparison of statistical probability for power larger than a preset value between the CME data sequence (asterisk *) and an artificially yet sufficiently randomized CME data sequence (+).

waves (Lou 1987, 2000b, 2001) may give rise to valuable periodic or quasi-periodic signatures from magnetized compact stars such as neutron stars and white dwarfs that are covered by corotating thin yet dense “plasma oceans” involving extremely strong magnetic fields ranging from 10^7 G to 10^{15} G . It is our desire to use the Sun as an astrophysical laboratory to search for, to identify, and to understand stellar Rossby-type waves.

2 DATA ANALYSIS AND RESULTS ON QUASI-PERIODICITIES

The time sequence of daily CME counts was derived from a preliminary list of *LASCO/SOHO* compiled by the Naval Research Laboratory (NRL) at the website lasco-www.nrl.navy.mil/cmelist.html. The solar X-ray flare data were taken from the *GOES* at the website www.ngdc.noaa.gov/stp/SOLAR/solar.html and from the website www.sec.noaa.gov/Data/solar.html. The data of the daily averaged Ap index for geomagnetic storm disturbances were obtained from the *WDC* of the *IAGA* at the website swdcdb.kugi.kyoto-u.ac.jp/wdc/Sec3.html.

2.1 Fourier Power Spectral Analyses

The uninterrupted data for daily counts of CMEs from *LASCO/SOHO* are displayed in Fig. 1a. Prior to Feb. 5, 1999, there were several unfortunate interruptions of *SOHO* operations and those earlier CME data are therefore excluded. Fig. 1b is the Fourier power spectrum of the data shown in Fig. 1a. In spite of the dominance (Fig. 1a and 1b), peak A at ~ 1101 -day period is not reliable as this period is not much less than the total data length of 1467 days (edge effects). While being preliminary, the next three significant peaks B, C, and D at quasi-periods of $\sim 358 \pm 38$, $\sim 272 \pm 26$, and $\sim 196 \pm 13$ days, respectively, are longer than the usual Rieger-type quasi-periods (Rieger et al. 1984; Dennis 1985; Sturrock & Bai 1992) in the flare-related data (see Table 1 for significant CME power peaks identified). To estimate possible errors in periods of identified power peaks, we take half of the full width at half maximum (FWHM) about a power peak in Fig. 1b as the angular frequency variation $\Delta\omega$. Then the period variation is given by $\Delta P = -P\Delta\omega/\omega$. That is, $P \pm \Delta P$ would give an estimated period variation range for an identified power peak. In the same manner, we have obtained estimates for power spectra of X-ray flares (class $>M5.0$) and of daily averages of Ap index (see Table 1 for details). By Table 1, ΔP increases with increasing P in general.

For time series of the daily CME data shown in Fig. 1, we took the following steps to estimate the statistical significance of Fourier spectral power peaks (e.g., Delache et al.

Table 1.

List of quasi-periodicities (Data sets from February 5, 1999 to February 10, 2003)

Item		Identified Quasi-Periods by Spectral Power Peaks in Unit of Days											
		A	B	C	D	E	F	G	H	I	J	K	L
CME	P	1101.22	358.33	271.99	195.88	110.80	100.00	66.25	60.64	57.26	35.85	33.49	20.62
	ΔP	671.48	37.68	26.22	13.38	3.26	2.88	1.31	0.90	1.00	0.40	0.39	0.17
Flares	P	1505.00	259.48	156.77	122.19	98.15	67.69	63.73	42.16	38.71	33.53		
	ΔP	589.46	24.23	10.89	4.88	3.25	2.18	2.34	0.78	0.55	0.52		
Ap	P	940.63	364.11	272.81	187.34	138.07	91.49	60.64	27.80	27.08	24.69	24.00	23.29
	ΔP	249.85	38.91	25.55	12.05	6.33	5.19	2.38	0.22	0.21	0.17	0.25	0.14

All original data were taken from February 5, 1999 to February 10, 2003. Significant power peaks based on Fourier analyses are identified and summarized here. We have periodicity = $P \pm \Delta P$ and $\Delta P = -P\Delta\omega/\omega$ where $\Delta\omega$ is a half of the full width at half maximum (FWHM) about a power peak. See Figs. 1, 2, and 3 in the text for CME, X-ray solar flares, and Ap index, respectively.

Figure 2. The same panel arrangement as in Fig. 1 but for the X-ray solar flare data (class $> M5.0$) from GOES during the same time span indicated on top.

Figure 3. The same panel arrangement as in Fig. 1 but for the daily averaged Ap index of geomagnetic disturbances from the WDC/IAGA during the same time span indicated on top.

1985). First, the daily CME data is picked at random within the time sequence and rearranged several to more than ten times to form an artificially randomized sequence (similar to the process of shuffling cards) with much reduced coherent periodic signals if any. For such a white noise sequence of independent Gaussian distributions with variance σ^2 , a Fourier transform would yield a power spectrum characterized by a probability distribution $p(w) = \exp[-w/(2\sigma^2)]$ for spectral powers greater than a preset value w . The approximate straight line of symbol + in Fig. 1c represents the natural logarithm of $p(w)$, $\ln[p(w)]$, versus w for an artificially randomized CME data sequence with a variance of $\sigma^2 \cong 1.46 \times 10^{-3}$ ($\sigma \cong 3.8 \times 10^{-2}$) estimated from the slope of this line. The relevant σ -levels of *fluctuation amplitudes* are then shown (viz., the two horizontal dashed lines in Fig. 1b corresponding to 3σ and 4σ levels as well as a sequence of numeral marks on top of Fig. 1c). Next, the natural logarithm of probability for spectral powers greater than a preset value w is estimated from the power spectrum of the actual daily CME counts (symbol * in Fig. 1c). A comparison of the two curves in Fig. 1c clearly indicates that for powers greater than the 3σ -level, the CME data starts to depart from random noises. Power peaks B through K in Fig. 1c are regarded as significant. Periods of peaks J and K are $\sim 36 \pm 0.4$ and $\sim 33 \pm 0.4$ days, respectively. We ran the same test procedure for the other two data sets and obtained qualitatively similar properties. That is, for both Ap index and X-ray solar flares of class $\gtrsim M5.0$ data sets examined below, deviations from random noises are also notable for power peaks $\gtrsim 3\sigma$ -level (see Figs. 2c and 3c).

It should be noted that such a procedure can be executed whatever the count distribution of the original data sequence may be. In fact, we have obtained data count dis-

tributions about the respective means for all three data sequences (i.e., CMEs, X-ray flares, and Ap index). It turns out that both CME and X-ray flare data more or less follow a Poisson distribution (that is, $P_\mu(\nu) = \exp(-\mu)\mu^\nu/\nu!$ where μ is the mean count rate and ν is the actual count rate; see e.g., Taylor 1981), while the Ap data deviate significantly away from a Poisson distribution (not surprisingly).

Entirely parallel to the panel arrangement of Fig. 1, Figure 2 presents a similar analysis on daily counts of X-ray solar flares of class $\gtrsim M5.0$ from the *GOES*. By Fig. 2c, the estimated variance is $\sigma^2 \cong 3.52 \times 10^{-5}$ ($\sigma \cong 5.9 \times 10^{-3}$). As a confirmation, the X-ray flare data in Fig. 2a does contain the familiar Rieger or Rieger-type quasi-periodicities $\lesssim 157 \pm 11$ days (see Fig. 2b and Table 1 for power peaks identified in the solar X-ray flare data) which do not have significant counterparts in the CME power spectrum except for periods of $\sim 34 \pm 0.5$, $\sim 39 \pm 0.6$, and $\sim 98 \pm 3$ days (Fig. 1b and Table 1). As we deal with the most powerful X-ray flares, this appears to be consistent, in trend, with the fact that Rieger-type quasi-periodicities were first discovered (Rieger et al. 1984) in γ -ray flares by the *SMM/GRS* followed by detections in soft X-ray flares (Kiplinger et al. 1984). Note that peak B of $\sim 259 \pm 24$ -day period appears significant enough ($> 4\sigma$ level) and may be related to the $\sim 272 \pm 26$ -day period in the CME data. For reasons noted earlier, peak A at 1505 ± 589 -day period again might not be reliable even though its apparent confidence level is merely slightly $\lesssim 95\%$.

Similarly, Figure 3 contains the relevant information of the daily averaged Ap index for geomagnetic storm disturbances, with an estimated variance $\sigma^2 \cong 0.08$ ($\sigma \cong 0.28$). Power peaks C and D in Fig. 3b at periods $\sim 273 \pm 26$ and $\sim 187 \pm 12$ days may correspond to the two peaks at periods $\sim 272 \pm 26$ and $\sim 196 \pm 13$ days of the CME data in Fig. 1b. There also exists a fairly prominent peak H ($> 4\sigma$ level) at a $\sim 28 \pm 0.2$ -day period. The $\sim 138 \pm 6$ -day period might correspond to the $\sim 157 \pm 11$ -day period in X-ray flare data; admittedly, this correspondence is somewhat weak given the ranges of error estimates. Should this correlation be real, then there might exist subclasses of geomagnetic disturbances which are proportionally correlated with major X-ray solar flares (class $> M5.0$). As already suspected, the 941 ± 250 -day period may not be reliable due to edge effects. In sharp contrast, by a visual inspection of Fig 3a and 3b, the most dominant power peak D at period

Figure 4. Period-time contours of Morlet wavelet analysis on the solar CME data (Feb 5, 1999 to Feb 10, 2003) with $\omega_0 = 6$ and the normalized power. Timescales (periods) of power peaks *A* through *E* are summarized in Table 2. The cone of influence (COI) is beneath the dashed curve.

Figure 5. Period-time contours of Morlet wavelet analysis on the X-ray solar flare data (class $> M5.0$) with $\omega_0 = 6$ and the normalized power. Timescales (periods) of power peaks *A* through *F* are summarized in Table 2. The cone of influence (COI) is beneath the dashed curve.

of $\sim 187 \pm 12$ days for Ap index should be physically real. In Fig 3, the prominent peak *H* around $\sim 28 \pm 0.2$ -day period in the daily averaged Ap index is physically identified with the solar rotation that recurrently brings high-speed solar wind streams from low-latitude coronal holes towards the Earth's magnetosphere. Note that this $\sim 28 \pm 0.2$ -day period is almost absent in the CME data.

2.2 Considerations of Statistical Significance

Figs. 1c, 2c, and 3c provide a sense of statistical significance for power peaks identified in the periodograms of CME, X-ray flare, and daily averaged Ap index data, respectively. Basically, when a spectral amplitude (square root of a power peak) becomes higher than the 3σ -level, the statistics of corresponding power peaks in the periodograms (asterisks *) starts to deviate from power peaks derived from randomized data series (crosses +). The higher the spectral amplitude, the larger the deviation in statistics.

Any one of the time series analyzed here contains random fluctuations that may not necessarily obey Gaussian distribution. The corresponding power spectrum naturally contains random variations. For independent daily counts of sufficiently large number in a data sequence, the corresponding Fourier amplitudes obey Gaussian distribution by the central limit theorem (e.g., Fan & Bardeen 1995). Therefore, the power probability distribution of $Z \equiv P(\omega)$ being in the interval $z < Z < z + dz$ is $Pr\{z < Z < z + dz\} = \exp(-z)dz$ where $P(\omega)$ is normalized by σ^2 . The cumulative distribution function is $Pr\{Z < z\} = \int_0^z \exp(-z')dz' = 1 - \exp(-z)$. Consequently, the probability for $Z > z$ is $Pr\{Z > z\} = \exp(-z)$. To search for the maximum value of power peaks among N independent frequencies such that Z are independent random variables, the corresponding probability is

$$Pr\{Z_{\max} > z\} = 1 - [1 - \exp(-z)]^N.$$

By this expression, it follows that a preset threshold $z = z_0$ for power peaks among N independent variables is related to the probability (false alarm probability p_0) that a peak, being produced randomly by chance, is greater than z_0 (Lomb 1976; Scargle 1982; Ballester et al. 2002).

To further assess the statistical significance of power peaks in Figs. 1 to 3 in this approach, we estimate the de-

Table 2. List of power peaks in Morlet wavelet contours

Item	Periods in Days for Contour Peaks					
	A	B	C	D	E	F
CMEs	343.0	187.0	102.0	38.3	36.1	
X-ray Flares	242.5	144.2	72.1	66.1	39.3	25.5
Ap index	288.4	187.0	66.1	51.0		

In normalized Morlet wavelet period-time contours of Fig. 4 (CME data), Fig. 5 (X-ray flare data), and Fig. 6 (Ap index data), we identify power peaks and timescales (periods) at the 99 percent confidence level (1 percent significance), respectively.

tection threshold $z_0 = -\ln[1 - (1 - p_0)^{1/N}]$ in spectral power with a false alarm probability p_0 , where N is the number of independent frequencies over which a power peak is searched for (Scargle 1982). In our case, $N = 734$ (a half of the total number of days of observations); for a false alarm probability $p_0 = 0.01$ (99% confidence), we have a detection threshold of $z_0 \cong 11.2\sigma^2$ and for $p_0 = 0.05$ (95% confidence), we have a detection threshold of $z_0 \cong 9.6\sigma^2$. In Fig. 1, peaks *B*–*D*, *F*, *G*, *J*, *K* are above the 99% confidence level; and peaks *E*, *H*, and *I* are above the 95% confidence level. In Fig. 2, peaks *B*–*E* and *H*–*J* are above the 99% confidence level. In Fig. 3, peaks *C*, *D*, *H*, *I*, and *J* are above the 99%; and peaks *B*, *F*, *G*, and *K* are above the 95% confidence level.

The tentative correlation found between mid-term quasi-periodicities of the CME and Ap data (Figs. 1 and 3) can be of physical significance. Besides the cause of recurrent high-speed solar winds with southward interplanetary magnetic fields for geomagnetic disturbances, a geomagnetic storm may set in when a CME or a part of a CME impinges upon the Earth's magnetosphere (Cane et al. 2000; Wang et al. 2002). ¹ Among all solar CMEs, there is certainly a significant fraction that miss the Earth's magnetosphere owing to their various initial onset orientations over the solar surface. Statistically, the probability, roughly proportional to the solid angle subtended by the Earth's magnetosphere towards the Sun, that CMEs hit the Earth's magnetosphere is higher for more frequent occurrence of CMEs. It is in this proportional sense that periodicities in CME and Ap data should correlate with each other. This is an important perspective for probing solar-terrestrial interactions and space weather conditions. This empirical correlation also strengthens our confidence that the two low-frequency power peaks *C* and *D* in the CME data are likely to be physically real.

The solar X-ray flare $\sim 259 \pm 24$ -day period is close to the CME $\sim 272 \pm 26$ -day period and the Ap $\sim 273 \pm 26$ -day period. If not coincidental by chance, this might indicate a certain causal relation among energetic X-ray solar flares ($\gtrsim M5.0$) and CMEs. Meanwhile, we caution that it would be premature to claim the existence of different types of solar flares associated with global CMEs.

Figure 6. Period-time contours of Morlet wavelet analysis on the Ap index data with $\omega_0 = 6$ and the normalized power. Timescales (periods) of power peaks *A* through *D* are summarized in Table 2. The cone of influence (COI) is beneath the dashed curve.

¹ For example, Jupiter's hectometric radio emissions and extreme ultraviolet aurorae were found to be triggered by arrivals of interplanetary shocks according to simultaneous observations of the Cassini and Galileo spacecraft (Gurnett et al. 2002).

2.3 Morlet Wavelet Analyses

As already noted earlier, mid-term quasi-periodicities of various solar flare related diagnostics may change for maxima of different solar cycles. It is thus of considerable interest to see whether such periodicities change within a few years around the maximum phase of a solar cycle. It is also important to check whether power peaks of Fourier spectral periods and of wavelet contour timescales have reasonable correspondence. For correlation studies of different time series data, it is crucial to know at what times certain periodicities occur or recur.

For these purposes, we perform wavelet analysis on the three time series for the CMEs, solar X-ray flares, and Ap index using the Morlet wavelet function

$$\psi_0(\eta) = \pi^{-1/4} e^{i\omega_0\eta} e^{-\eta^2/2} \quad (1)$$

where $\omega_0 = 6$ is chosen. The Fourier time period τ and the Morlet wavelet timescale s are related by

$$\tau = 4\pi s/[\omega_0 + (2 + \omega_0^2)^{1/2}] \quad (2)$$

(see Table 1 of Torrence & Compo 1998). For our choice of $\omega_0 = 6$, it follows from equation (2) that $\tau = 1.033s$, namely, Fourier periods and Morlet wavelet timescales are nearly equal to each other. The wavelet transform suffers from edge effects at both ends of the time series. This gives rise to a cone of influence (COI) as indicated by regions below the dashed lines in Figures 4, 5, and 6. Caused by padding zeroes at the beginning and at the end of data series, these edge effects usually lead to a power reduction within the COI. For further detailed technical information of Morlet wavelet analysis, one may visit the website at <http://paos.colorado.edu/research/wavelets/wavelet2.html>.

At the 99 percent confidence level (1 percent significance) and using the Morlet wavelet function defined by equation (1), contour plots in period-time (or equivalently, scale-time) domains with color coding are shown for the CME, X-ray solar flares, and Ap index data in Figures 4, 5, and 6, respectively, and corresponding contour peaks are summarized in Table 2.

Comparing Table 1 and Table 2, we find that CME Fourier periods B , D , F , and J at $\sim 358 \pm 38$, $\sim 196 \pm 13$, $\sim 100 \pm 3$, and $\sim 36 \pm 0.4$ days roughly correspond to CME Morlet periods A , B , C , and E at ~ 343 , ~ 187 , ~ 102 , and ~ 36 days, respectively; X-ray flare Fourier periods B , C , F , and I at $\sim 259 \pm 24$, $\sim 157 \pm 11$, $\sim 68 \pm 2$, and $\sim 39 \pm 0.6$ days roughly correspond to X-ray flare Morlet periods A , B , C , and E at ~ 243 , ~ 144 , ~ 66 , and ~ 39 days, respectively; and Ap index Fourier periods C , D , and G at $\sim 273 \pm 26$, $\sim 187 \pm 12$, and $\sim 61 \pm 2$ days roughly correspond to Ap index Morlet periods A , B , and C at ~ 288 , ~ 187 , and ~ 66 days, respectively.

The most prominent match is the ~ 187 -day period in both CME and Ap index data (this quasi-periodicity is also present in corresponding Fourier power spectra). As already noted earlier, we suspected that this Ap index periodicity was driven by periodic CMEs. These comparisons suggest that CMEs and Ap index for geomagnetic disturbances may proportionally correlate with each other in both periods and time. We categorically emphasize that power peaks in Ap index data around $181 - 187$ days are so prominent in Figs. 3a, 3b, and 6, and that they should be physically real for

whatever origin. Here, the evidence lends support for the CME-driven scenario in the statistical sense.

Wavelet power peak in C–D range of Fig. 6 (Ap index) and wavelet power peak in C–D of Fig. 5 (X-ray flares) have comparable timescales of ~ 66 days. They occur around the same time and may be interpreted as flare-driven periodicities in Ap index data. There is also a match around periodicity of ~ 39 days in both X-ray flare and Ap index data. However, there is a time difference for the two relevant power peaks in CME and X-ray flare data. From such information alone, correlations between solar X-ray flares and CMEs at these timescales are not immediately clear.

2.4 A Test of Incomplete X-Ray Flare Data

Such CME mid-term quasi-periodicities (present in both Fourier spectrum and Morlet wavelet analyses), if confirmed by further independent observations, offer novel diagnostics for probing and understanding the physical origin of CMEs (e.g., Hundhausen 1999; Low 2001). Up to this point, one major question arising from our comparative data analysis is that there are mid-term quasi-periodicities in the *LASCO/SOHO* data for CMEs but these periodicities, except for a few, are largely independent of the Rieger-type quasi-periodicities detected in various phenomena associated with energetic X-ray solar flares.

While the *SOHO/LASCO* data of CMEs including all halo events is the most complete one, the X-ray solar flare data of the *GOES* suffer incompleteness because one cannot see the other half of the Sun at any given moment. Might this be the cause of differences in some quasi-periodicities seen in CMEs and solar X-ray flares? We designed a simple test to address this issue with the assumption that a strong X-ray solar flare occurs at one footpoint of a CME. In this scenario, a CME may be related to one flare at most. For example, we may observe a CME without seeing an intense X-ray flare perhaps because one footpoint of the CME is located on the frontside but another is located on the backside of the Sun and the corresponding flare happens at the footpoint on the backside. By all combinations, M CMEs per day may correspond to $M + 1$ ($0, 1, \dots, M$) possible X-ray flare counts on the frontside of the Sun. Based on the CME data, we then rely on a random number generator to select one of the possibilities as observable flare events per day. The key features of the resulting power spectrum thus obtained do not change significantly for arbitrary trials. This test seems to indicate that should a more complete data set of solar flares be available, the major quasi-periodic features in the power spectrum would remain.

3 MID-TERM QUASI-PERIODICITIES

On the basis of our data analyses reported here, it appears that, with high probability, mid-term quasi-periodicities do exist in association with diagnostics of various solar activities (CMEs and X-ray solar flares) as well as geomagnetic disturbances (Ap index). Some of the overlapping quasi-periodicities might reveal underlying physical causes. We shall discuss qualitatively plausible physical connections.

3.1 Quasi-Periodicities in Flux Emergence

Regarding the theoretical suggestion of equatorially trapped Rossby waves (Lou 2000a, b) for Rieger-type periodicities in flare-related diagnostics, we note that intuitively, solar flare rate and emergence of complex magnetic regions of sunspots or sunspot groups should relate to each other in a statistically correlated manner (Oliver et al. 1998; Ballester et al. 1999, 2002). Empirically, nearly all solar flares are found close to sunspots or sunspot groups and often seen as brightenings of the pre-existing plages; the observed quasi-periodicities (Bai 1992; Oliver et al. 1998) in sunspot areas or number of sunspot groups do indeed correlate with those of flare occurrence rates. Is this merely a coincidence? Or, does this actually hint at an underlying global mechanism? We here discuss two seemingly independent aspects, namely, the emergence of magnetic fluxes and the occurrence of solar flares, even though the two aspects should in some sense be related to each other empirically.

Whether magnetic fields are generated deep in the Sun's radiative interior (e.g., Gough & McIntyre 1998) or at the bottom of the solar convection zone (e.g., Rosner & Weiss 1985), some of these magnetic fluxes must somehow float upward through the convection zone and eventually break through the thin photosphere by magnetic buoyancy (Parker 1955, 1979) to buckle upwards above the solar surface, forming sunspot pairs or groups. In the absence of a global quasi-periodic modulation mechanism, such process of magnetic flux emergence should be completely random. The observed quasi-periodicities in magnetic flux emergence would be consistent with (though by no means necessary) the presence of large-scale Rossby-type waves of comparable periodic timescales. Generally speaking, equatorially trapped Rossby-type waves (Lou 2000a, b) can dynamically affect subsurface as well as emerged large-scale magnetic fields (e.g., magnetic active regions) through squeezing, twisting, stretching and vortical motions, even though spatial scales of (emerged) individual sunspots or sunspot groups are relatively small.² More specifically, such equatorially trapped Rossby-type waves may tip off vulnerable regions for the onset of magnetic buoyancy instabilities via dynamic couplings. This plausibly links quasi-periodicities detected in sunspot areas or number of sunspot groups (Lean 1990; Oliver et al. 1998; Ballester et al. 1999, 2002) with equatorially trapped Rossby-type waves.

3.2 Quasi-Periodicities in Flare Diagnostics

The occurrence of solar flares involves sudden releases or bursts of considerable magnetic energies accumulated over a certain period of time (e.g., Parker 1979). It is almost impossible to predict the location and time of a solar flare.³ As magnetic fields associated with sunspots or sunspot groups are strong in strengths and complicated in structures, it is

² The process leading to the formation of such intense magnetic structures is nonlinear and complicated (Parker 1955).

³ This situation is analogous to hurricanes, earthquakes, and tornadoes in that vulnerable environments for their occurrences can be identified with relative ease while their specific occurrence location and time are very difficult to pinpoint or predict.

quite natural to somehow have a significant amount of magnetic energy stored in special ways as magnetic fields gradually evolve in time (Low & Lou 1990; Lou 1992). In contrast to nanoflares (Parker 1994) which frequently release magnetic energies on smaller scales (e.g., X-ray bright points) for heating the lower corona, this accumulation (or storage) stage of magnetic energies is necessary for flare phenomena in general otherwise solar flares would not be so violent and explosive (e.g., Zirin 1988). At critical moments, small disturbances of whatever origin may *trigger* magnetic avalanches, leading to productions of energetic particles and wide-spectrum electromagnetic radiations. Only in this sense, a sustained passage of Rossby-type waves can increase *statistically* the chance of flare occurrence in pre-existing vulnerable magnetic complexes and thus impose quasi-periodicities to various diagnostics associated with X-ray solar flares.

3.3 Dynamic Feedback Cycle

Having argued heuristically about possible roles of equatorially trapped Rossby-type waves in triggering the emergence of magnetic fluxes and the onset of solar flares in a statistically correlated manner, we need to address the pressing question of Rossby-type wave excitation (Lou 2000a, b). Whether such waves (with much weaker magnitudes) exist or not during the solar minimum phase is not presently known. Nevertheless, preceding discussions require their presence as a large-scale coordinating mechanism during the solar maximum phase.

As a solar flare or a CME goes off, a fraction of their energies will back react on the solar photosphere and appear in the form of traveling disturbances. Collectively, a fraction of total flare or CME energies may provide a necessary energy source for generating and sustaining equatorially trapped Rossby-type waves during a few years around solar maxima. In this scenario, a *dynamic feedback cycle* may be established to sustain quasi-periodicities in magnetic flux emergence and flare activities. Failure of sustaining such a feedback cycle leads only to *occasional* periodicities in flare activities (see Fig. 5). This may explain why during maxima of some solar cycles, the 150-day quasi-periodicity becomes so prominent (Oliver et al. 1998) while in others it could be almost absent with yet different periodicities more overwhelming (cf. Bai 1992; Bai & Sturrock 1991, 1993; Sturrock & Bai 1992) — the dominant periodicity can be different during solar maxima of different solar cycles (e.g., Bai & Sturrock 1991; Bai 1992) and for different diagnostics (Oliver et al. 1998; Ballester et al. 1999, 2002). Fig. 5 clearly shows time variations of periodicities even within a few years of the recent solar maximum phase (cycle 23). This proposed feedback scenario leaves considerable rooms for possible correlations among intensities/rates of solar flares, selection of periodicities, and distribution of sunspot groups on both northern and southern sides of the solar equator during solar maxima and therefore also requires further explorations.

3.4 Quasi-Periodicities in CME Diagnostics

CMEs from the solar limb have been routinely monitored by various coronagraph observations (cf. Hundhausen 1999

for SMM results). With the ongoing Solar and Heliospheric Observatory (SOHO) mission in space, even relatively weak CME halo events⁴ can now be readily detected as well. By combining SOHO and ground-based observations, it is possible to construct a fairly complete time sequence for CMEs occurrence.

CMEs represent a major class of large-scale solar activities involving magnetic field and perhaps sub-photospheric magnetic flux emergence. Physically, CMEs are characterized by large-scale eruptive mass losses from the Sun into the solar wind (Hundhausen 1999) and are thought to be caused by a sudden loss of magnetic equilibria (Low 1990) as photospheric magnetic field structures evolve gradually in time. The primary energetics of CMEs is believed to be magnetic in nature. At a critical stage of large-scale magnetic structure evolution, a CME may be *triggered* by disturbances. As a systematic and quasi-periodic source of large-scale disturbances at the photospheric level, equatorially trapped Rossby-type waves may modulate CMEs in a periodic yet statistical manner.

4 APPLICATION OF ROSSBY-TYPE WAVES

Our comparative observational research is motivated by the known mid-term quasi-periodicities, namely, Rieger-type periodicities, in various solar flare related diagnostics and our analysis here on X-ray flares (class $> M5.0$) during the recent solar maximum of cycle 23 confirms once again the existence of such Rieger-type periodicities. What is then the underlying physics for such “discrete quasi-periods” arranged roughly like subharmonics and significantly longer than the solar rotation period if they are indeed real? Solely from the perspective of period matchings, it appears that solar Rossby-type waves are the best bet for such discrete subharmonic quasi-periodicities, although many questions remain to be addressed for this proposal (Lou 2000a, b).

Now given the global nature as well as randomness of CME events, how does one infer the underlying physics for mid-term quasi-periodicities (see Fig. 1 and Table 1) longer than those of the Rieger type? The reality of such mid-term quasi-periodicities for CMEs appears to be indirectly supported by the presence of similar quasi-periodicities in the daily average of Ap index (see Fig. 3 and Table 1). The basic rationale for such a remote connection is that quasi-periodic CMEs should lead to quasi-periodic geomagnetic disturbances when a fraction of CMEs encounter the Earth’s magnetosphere. It is certainly possible to match the identified quasi-periods of CMEs with periods of Rossby-type waves (Lou 2000a, b) as we did for Rieger-type periodicities. However, as shown in Table 1, longer periods have larger error ranges comparable to the equatorial solar rotation period, that is, the accuracy is insufficient to warrant a one-to-one correspondence without ambiguities.

With these qualifications and limitations in mind, we shall nevertheless discuss several empirical, intuitive and conceptual aspects of mid-term quasi-periodicities in reference to equatorially trapped Rossby-type waves.

⁴ The strengths of these halo CMEs are not necessarily weak. They are not as easy to detect merely because they originate somewhere within the solar disk.

For Rieger-type periodicities, we may estimate the quasi-periods of equatorially trapped Rossby-type waves by taking $m = 12, 10, 8, 6$ and 4 with $n = 1$ or 2 in expressions (13) and (15) of Lou (2000b). We suspect that the spatial distribution of sunspot groups or active regions along the equatorial zone might be one important factor in the selection of the two integers m ($k_x \equiv m/R_\odot$ is the azimuthal wavenumber) and n (number of nodes for a Rossby wave function along a longitude) during the solar maximum phase. By definition, a solar minimum is characterized by a fewer number of sunspots and thus less activities. During a solar maximum in contrast, radio images of the Very Large Array (VLA) as well as X-ray images from Yohkoh reveal two quasi parallel chains of 5 or 6 emission-intense “blobs” from sunspot groups or magnetic complexes on both northern and southern hemispheres.⁵ As these “blobs” are sites of frequent flare occurrence, excited equatorially trapped Rossby-type waves are likely to concentrate their powers in the relevant m which roughly corresponds to the number of “blobs” around the Sun. For ~ 5 or 6 active centers in the solar disk facing us, m would then be ~ 10 or 12 around the circumference. In turn, Rossby-type wave disturbances will statistically trigger more flares in active regions. In essence, this is part of the dynamic feedback cycle outlined earlier.

Likewise, the gross symmetry for the numbers of active regions across the equator would correspond to $n = 2$. Thus, equatorially trapped Rossby-type waves with $n = 2$ might be favorably excited given the presence of two belts of sunspot groups across the equator. It should be noted that for wave modes with even n , the north and south are symmetric with respect to the equator; and for wave modes with odd n , the north and south are antisymmetric with respect to the equator. Of course, for a mixture of Rossby-type wave modes with both odd and even n , it is not possible to identify a symmetry with respect to the equator in the strict sense.

Observationally, the distribution of active regions is sometimes not grossly symmetric with respect to the equator during a certain epoch of a solar maximum phase and this situation may correspond to odd values of n . This might be the cause of north/south asymmetries sometimes observed in periodicities of flare rates (e.g., Bai 1987). One should keep in mind that for $n = 1$ or 2 and $m \geq 4$, the angular wave pattern speeds $\omega_p \equiv \omega/m$ of equatorially trapped Rossby-type waves are approximately proportional to $\sim 2\Omega_\odot/m^2$. The larger the value of m , the slower the angular wave pattern speed ω_p . By including effects of surface elevation (see equations 1-3 of Lou 2000), periods of Rossby-type wave crest bumping into the next adjacent active region are $2\pi/|m\omega_p|$ as specifically given by expressions (13) and (15) of Lou (2000b), namely,

$$P_r \cong P_\odot \{ |m|/2 + (2n+1)\Omega_\odot R_\odot / [|m|(gD)^{1/2}] \} \quad (3)$$

for Rossby-wave periods, and

$$P_{r-p} \cong \{ |m| + [m^2 + 8\Omega_\odot R_\odot / (gD)^{1/2}]^{1/2} \} P_\odot / 4 \quad (4)$$

for Rossby-Poincaré-wave periods, respectively, where $P_\odot \equiv$

⁵ In some cases, the separation of different “blobs” may involve certain ambiguities. Sometimes, one might hesitate as whether to count a “blob” at the limb or not. For the present purpose, we mainly focus on the basic concept of such mode selection.

$2\pi/\Omega_\odot$ is the Sun's sidereal rotation period, $\Omega_\odot R_\odot \sim 2 \text{ km s}^{-1}$ is the equatorial solar rotation speed and $(gD)^{1/2}$ is the solar surface gravity wave speed with $g \sim 2.7 \times 10^4 \text{ cm s}^{-2}$ being the solar surface gravity and D (of a few hundred kilometers) being an effective thickness of the photospheric layer.

The solar photosphere is magnetized with well-known inhomogeneities on smaller scales such as concentrations of intense magnetic fibrils ($\sim 10^3 \text{ G}$) along boundaries of supergranules whose typical diameters are on the order of $\sim 3 \times 10^9 \text{ cm}$ and appearances of sunspots or sunspot groups (of sizes comparable to that of a typical supergranule) with magnetic field strengths up to $3 - 4 \times 10^3 \text{ G}$. Subsurface horizontal magnetic fields B_h (e.g., Babcock & Babcock 1955) may well be patchy on large scales of the order of $L \sim R_\odot$ and might be fairly strong deep in the solar interior (e.g., Gough & McIntyre 1998). However, as the gas density ρ increases rapidly with depth by gravitational stratification, the value of the Alfvén wave speed $C_A \equiv B_h/(4\pi\rho)^{1/2}$ may not be very large (say, $C_A \lesssim$ a few km s^{-1} in the overshoot layer suspected to be strongly magnetized).

In terms of large-scale magnetohydrodynamic (MHD) wave propagations in a thin layer with a relatively small C_A and a relatively large azimuthal perturbation scale, the role of subsurface magnetic field B_h may be crudely assessed (Lou 1987). The presence of B_h introduces a large-scale horizontal magnetic pressure force in addition to the quasi-hydrostatic pressure force $\rho g \eta$ caused by the surface elevation η and thus effectively increases the surface wave speed in the form of $c_L \sim (gD + C_A^2)^{1/2}$ where $D \lesssim 500 \text{ km}$ is an estimated photospheric layer thickness and $g = 2.7 \times 10^4 \text{ cm s}^{-2}$ is the solar surface gravity. Replacing the surface wave speed $c \equiv (gD)^{1/2}$ by c_L here, expressions (7) and (11) of Lou (2000b) then give increased frequencies of equatorially trapped Kelvin- and Poincaré-waves (thus shorter periods than a couple of days), whereas expressions (13) and (15) of Lou (2000b) (or equations (3) and (4) here) show that the frequencies of equatorially trapped Rossby-type waves remain more or less unchanged because they are primarily determined by the solar rotation rate Ω_\odot and the minor correction term involves the speed ratio $\Omega_\odot R_\odot/(gD + C_A^2)^{1/2}$ which is reduced further by the presence of B_h . For Rossby-type waves, this allows *more* nearby frequencies to be packed into the frequency groups labeled by m with different values of n .

5 OTHER CIRCUMSTANTIAL EVIDENCE FOR ROSSBY-TYPE WAVES

While solar Rossby-type waves or r -modes have been proposed along several lines of research (Papaloizou & Pringle 1978; Wolff 1998; Lou 1987, 2000a, b), there is no direct solid evidence so far for their detection at the solar photosphere except for a few tantalizing cases discussed below. We intend to stimulate further investigations of this problem both observationally and theoretically.

The velocity correlation analysis on the data from the *Solar Oscillation Investigation/Michelson Doppler Imager (SOI/MDI)* revealed stationary "long-lived velocity cells" (Beck et al. 1998) located along the solar equatorial zone. In terms of horizontal surface velocities (a few meters per sec-

ond) and spatial scales ($\sim 50^\circ$ in longitude), it is inevitable on theoretical ground that such large-scale "velocity cells" should travel in the form of Rossby-type waves relative to the Sun at speeds slower than the solar rotation (Lou 1987, 2000a, b). An azimuthal scale of $\sim 50^\circ$ may correspond to an azimuthal wave integer $m = 6$ or 7 which would give an equatorially trapped Rossby wave period $\gtrsim 77$ but $\lesssim 102$ days (Lou 2000b). The diagnostic approach of Beck et al. (1998) is promising, although more sophisticated velocity correlation analyses of the *SOI/MDI* data are required in order to extract signals of large-scale, slowly drifting Rossby-types wave patterns over the solar photosphere.

Using the solar limb data from the *SOI/MDI*, Kuhn et al. (2000) reported periodic signals of 100 m high "hills" that are separated by an azimuthal scale of $(8.7 \pm 0.6) \times 10^4 \text{ km}$. Note that this surface elevation of $\sim 100 \text{ m}$ is some 700 times smaller than the upper limit of $0.1''$ estimated by Lou (2000b). Uncertainties in such an estimate involves the effective thickness D of the solar photosphere and the extent of partial cancellations in the horizontal velocity divergence $\nabla_\perp \cdot \vec{v}_\perp$. The more precise result of Kuhn et al. (2000) casts serious doubts on earlier attempted measurements of variations in the solar diameter (e.g., Delache et al. 1985; Ribes et al. 1987; Yoshizawa 1999). If such solar limb elevations are indeed induced by Rossby waves with an azimuthal wave integer $m = 50$, then the corresponding equatorially trapped Rossby wave drifts at an extremely slow speed relative to the Sun with a period of ~ 625 days. It is somewhat surprising that limb elevations caused by Rossby-type waves with smaller values of m were not detected by the same technique of Kuhn et al (2000).

Combining the data from the *SOI/MDI* and the *Global Oscillation Network Group (GONG)*, Ulrich (2001) obtained persistent patterns of torsional oscillations with azimuthal structures characterized by $1 < m \lesssim 8$ yet without detecting signals of quasi-periodicities. For this range of m values, periods of equatorially trapped Rossby waves should lie in the range of $\sim 27 - 102$ days (Lou 2000b). It is a challenge through a helioseismological data analysis to identify unambiguously signatures of solar Rossby waves that involve large-scale and long-lived structures of flow velocity and surface elevation over the slowly rotating solar photosphere.

Ballester et al. (2002) recently examined several historical records of solar photospheric magnetic fluxes. These records include (1) the Mount Wilson total magnetic flux (MWTF) from 1966 to 2000 for total daily magnetic flux measured in units of 10^{22} Mx , (2) the Kitt Peak magnetic flux (KPMF) from 1975 to 2000 in units of 10^{22} Mx in regions with magnetic field strength greater than 25 G within the latitude band S70°-N70°, and (3) the daily magnetic plage strength index (MPSI) and the Mount Wilson sunspot index (MWSI) from 1970 to 2000. They derived both periodogram and wavelet contours. The results of their data analysis show a near 160-day periodicity in the photospheric magnetic flux during solar cycle 21 (but not in solar cycle 22) and suggest a probable causal relation to the well-known Rieger-type quasi-periodicities. Given our data analyses on mid-term quasi-periodicities in CMEs and solar X-ray flares, it is very likely that during the recent solar maximum (cycle 23), the daily total solar magnetic flux of the MWTF, for example, should reveal Rieger-type periodicities. The results of Ballester et al. (2002) are consistent with the notion that

the emergence of subphotospheric magnetic flux may be triggered or modulated quasi-periodically by large-scale Rossby waves trapped in the solar equatorial zone (Lou 2000b).

6 DISCUSSION AND SUMMARY

In terms of the interrelation between mid-term quasi-periodicities of equatorially trapped Rossby waves and Rieger-type periodicities in solar flare related activities, we would offer several physical ideas here to address the interesting questions raised by Ballester et al. (2002) regarding the mechanism proposed by Lou (2000b). Due to the solar differential rotation, subsurface mean magnetic fields are wrapped around the solar equator with growing intensities. By turbulent convections and MHD instabilities, subsurface magnetic fluxes will emerge in general and sunspots or sunspot groups will form in particular. Magnetic activities above the photosphere are capable of disturbing the photosphere and sub-photospheric layers through MHD processes.

We thus have in mind a “dynamic feedback scenario” advanced earlier. Specifically, powerful solar flares frequently occurring in magnetic active regions along the two usual belts across the solar equator keep stirring the photosphere and exciting Rossby waves that in turn either trigger or modulate the emergence of subphotospheric magnetic flux. To sustain such a “dynamic feedback cycle”, initiations and positive feedbacks above a certain energetic “threshold” are necessary. This may explain why Rieger-type periodicities in the emergence of magnetic flux, sunspot areas, and high-energy flares etc. are detected within a few years around the solar maxima when solar activity levels are high. This also implies possible changes in the most dominant periodicities with different physical conditions for different solar maxima.

Practically, however, it is not easy to estimate this “threshold”, because several unknown parameters and processes are involved. Regarding possible values of m and n in the solar Rossby wave theory of Lou (2000b), we already noted that for ~ 5 or 6 active regions in the solar disk facing us, m would be ~ 10 or 12 around the circumference. Similarly, equatorially trapped Rossby-type waves with $n = 2$ may be more favorably excited given the presence of two belts of sunspot groups north and south of the equator. In the sense of triggering magnetic avalanches, a sustained passage of Rossby-type waves can increase *statistically* the chance of flare occurrence in preexisting vulnerable magnetic complexes and thus impose grossly quasi-periodicities to various diagnostics associated with solar flares.

In summary, by Fourier spectrum and Morlet wavelet analyses, we identified quasi-periods in data series of CMEs, X-ray solar flares (class $> M5.0$), and daily averages of Ap index during the time span from February 5, 1999 to February 10, 2003 for the solar maximum of cycle 23. CME periods at $\sim 358 \pm 38$, $\sim 272 \pm 26$, and $\sim 196 \pm 13$ days appear to correspond well to Ap index periods at $\sim 364 \pm 39$, $\sim 273 \pm 26$, and $\sim 187 \pm 12$ days, although the Ap index period of $\sim 364 \pm 39$ days is somewhat less significant; we interpret these quasi-periodic correlations in terms of CME interactions with the Earth’s magnetosphere. In addition to a significant period at $\sim 259 \pm 24$ days, X-ray flare data contains the familiar Rieger-type periodicities shorter than $\sim 157 \pm 11$ days and so forth. Within error ranges, this $\sim 259 \pm 24$ -day period in

X-ray flare data may relate to CME $\sim 272 \pm 26$ -day and Ap $\sim 273 \pm 26$ -day periods. We provide estimates for periodic timescales of equatorially trapped Rossby-type waves based on the work of Lou (2000a, b) and discuss a few qualitative aspects of a “dynamic feedback cycle” to sustain such waves. A coherent picture for solar Rossby waves is yet to come given several preliminary results of their circumstantial detections in recent years (Beck et al. 1998; Kuhn et al. 2000; Ulrich 2002). More observations and theoretical investigations are needed to further understand these mid-term quasi-periodicities in solar as well as solar-terrestrial activities.

Finally, we emphasize the strong obvious periodicity of 187 ± 12 -days in daily averaged Ap index that can be visually picked out in Fig. 3a. We tentatively identified a CME counterpart of period 196 ± 13 days as the cause. A further understanding of this phenomenon is of great interest especially in contexts of solar terrestrial interaction.

ACKNOWLEDGMENTS

This research (Y.Q.L.) was supported in part by grants from US NSF (AST-9731623) to the University of Chicago, by the ASCI Center for Astrophysical Thermonuclear Flashes at the University of Chicago under Department of Energy contract B341495, by the Special Funds for Major State Basic Science Research Projects of China, by the Collaborative Research Fund from the NSF of China for Outstanding Young Overseas Chinese Scholars (NSFC 10028306) at the National Astronomical Observatories, Chinese Academy of Sciences, and by the Yangtze Endowment from the Ministry of Education through the Tsinghua University. Affiliated institutions of Y.Q.L share this contribution. Z.H.F. was supported in part by the NSFC grant 10243006 and the Ministry of Science and Technology of China under grant TG1999075401.

REFERENCES

- Babcock H. W., Babcock H. D., 1955, ApJ, 12, 349
- Bai T., 1987, ApJ, 318, L85
- Bai T., 1992, ApJ, 388, L69
- Bai T., Cliver E. W., 1990, ApJ, 363, 299
- Bai T., Sturrock P. A., 1987, Nature, 327, 601
- Bai T., Sturrock P. A., 1991, Nature, 350, 141
- Bai T., Sturrock P. A., 1993, ApJ, 409, 476
- Ballester J. L., Oliver R., Baudin F., 1999, ApJ, 522, L153
- Ballester J. L., Oliver R., Carbonell M., 2002, ApJ, 566, 505
- Beck J. G., Duvall Jr., T. L., Scherrer P. H., 1998, Nature, 394, 653
- Bogart R. S., Bai T., 1985, ApJ, 299, L51
- Cane H. V., Richardson I. G., von Rosenvinge T. T., 1998, Geophys. Res. Lett., 25, 4437
- Cane H. V., Richardson I. G., St. Cyr O. C., 2000, Geophys. Res. Lett., 27, 3591
- Carbonell M., Ballester J. L., 1990, A&A, 238, 377
- Delache Ph., Laclare F., Sadsoud H., 1985, Nature, 317, 416
- Dennis B. R., 1985, Solar Phys., 100, 465
- Dröge W., Gibbs K., Grunsfeld J. M., Meyer P., Newport B. J., 1990, ApJS, 73, 279
- Fan Z. H., Bardeen J. M., 1995, Phys. Rev. D., 51, 6714
- Gilman P. A., 1969, J. Atmos. Sci., 26, 1003

Gilman P. A., Fox P. A., 1999, ApJ, 522, 1167

Gough D. O., McIntyre M. E., 1998, Nature, 394, 755

Gurnett D. A., et al., 2002, Nature, 415, 985

Hundhausen, A. 1999, in *The Many Faces of the Sun: A Summary of the Results from NASA's Solar Maximum Mission*, ed. by K. T. Strong, J. L. R. Saba, B. M. Haisch, & J. T. Schmelz (New York: Springer), 143

Ichimoto K., Kubota J., Suzuki M., Tohmura I., Kurokawa H., 1985, Nature, 316, 422

Kile J. N., Cliver E. W., 1991, ApJ, 370, 442

Kiplinger A. L., Dennis B. R., Orwig L. E., 1984, BAAS, 16, 891

Kuhn J. R., Armstrong J. D., Bush R. I., Scherrer P., 2000, Nature, 405, 544

Lean J. L., 1990, ApJ, 363, 718

Lean J. L., Brueckner G. E., 1989, ApJ, 337, 568

Lomb N. R., 1976, Ap&SS, 39, 447

Lou Y. Q., 1987, ApJ, 322, 862

Lou Y. Q., 1992, ApJ, 395, 682

Lou Y. Q., 2000a, BAAS, SPD-32.0502L

Lou Y. Q., 2000b, ApJ, 540, 1102

Lou Y. Q., 2001, ApJ, 563, L147

Low B. C., 1990, ARA&A, 28, 491

Low B. C., 2001, J. Geophys. Res., 106, 25,141

Low B. C., Lou Y. Q., 1990, ApJ, 352, 343

Oliver R., Ballester J. L., Baudin F., 1998, Nature, 394, 552

Özgüç A., Ataç T., 1989, Solar Phys., 123, 357

Pap J., Tobiska W. K., Bouwer S. D., 1990, Solar Phys., 129, 165

Papaloizou J., Pringle J. E., 1978, MNRAS, 182, 423

Parker E. N., 1955, ApJ, 121, 491

Parker E. N., 1979, *Cosmic magnetic fields: their origin and their activity* (New York: Oxford University Press)

Parker E. N., 1994, *Spontaneous Current Sheets in Magnetic Fields* (New York: Oxford University Press)

Provost J., Berthomieu G., Rocca A., 1981, A&A, 94, 126

Ribes E., Merlin Ph., Ribes J.-C., Barthalot R., 1987, *Annales Geophysicae* 7, 321

Rieger E., Share G. H., Forrest D. J., Kambach G., Reppin C., Chupp E. L., 1984, Nature, 312, 623

Rosner R., Weiss N. O., 1985, Nature, 317, 790

Rossby C.-G., et al., 1939, J. Marine Res., 2, 38

Saio H., 1982, ApJ, 256, 717

Scargle J. D., 1982, ApJ, 263, 835

Sturrock P. A., Scargle J. D., Walther G., Wheatland M. S., 1999, ApJ, 523, L177

Sturrock P. A., Bai T., 1992, ApJ, 397, 337

Taylor J. R., 1981, *An Introduction to Error Analysis* (Mill Valley, CA: University Science Books)

Torrence C., Compo G. P., 1998, Bull. Am. Meteor. Soc., 79, 61

Ulrich R. K., 2001, ApJ, 560, 466

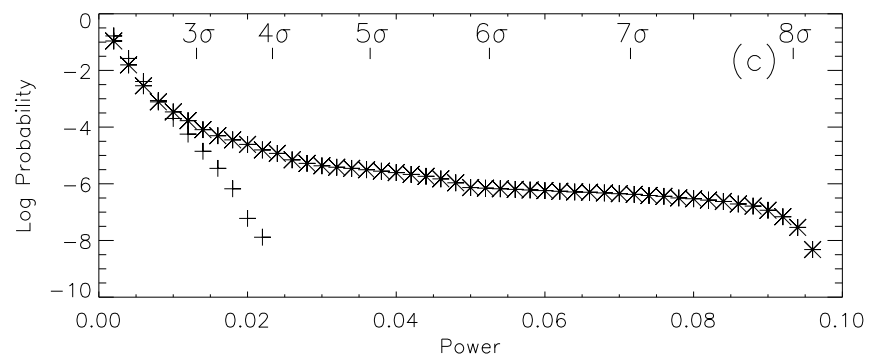
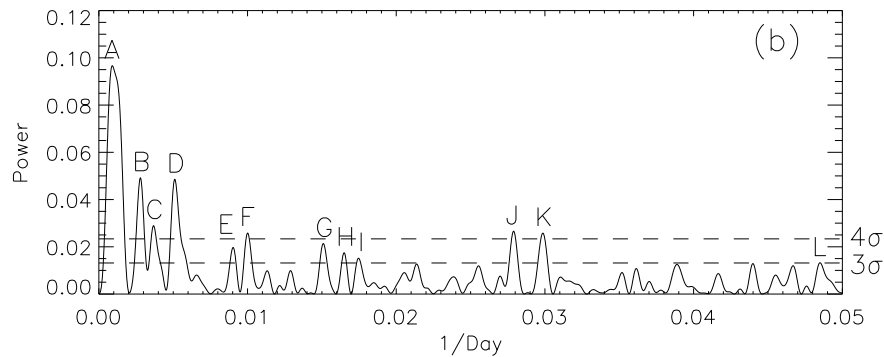
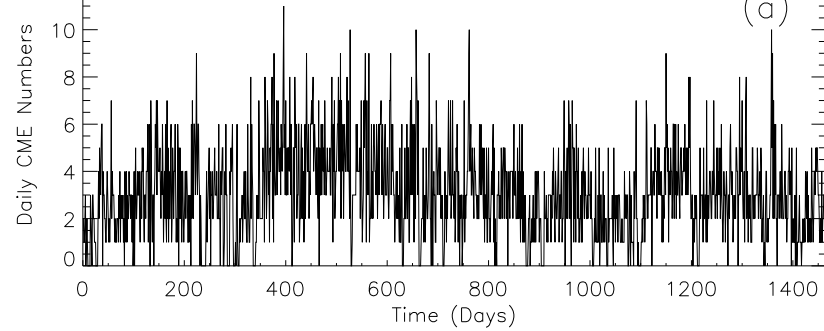
Verma V. K., Joshi G. C., Paliwal D. C., 1992, Solar Phys., 138, 205

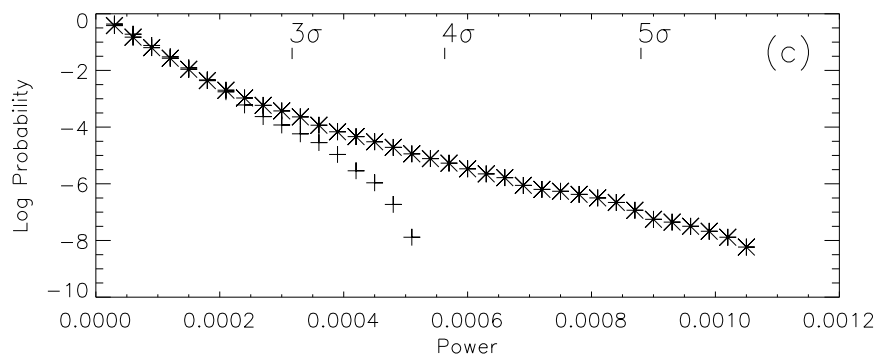
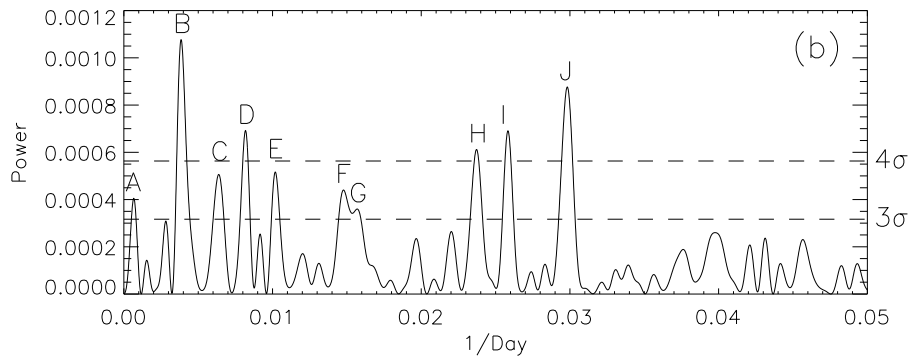
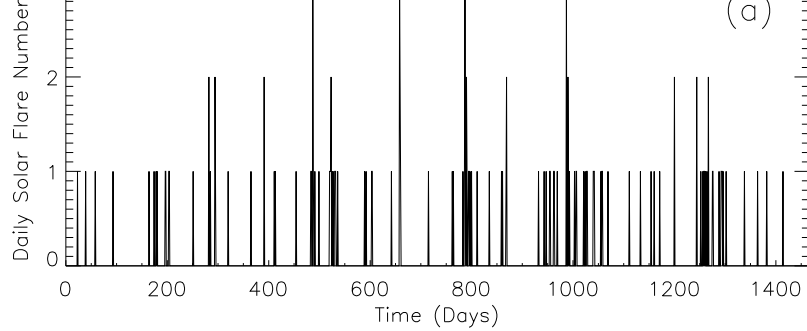
Wang Y. M., Ye P. Z., Wang S., Zhou G. P., Wang J. X. 2002, J. Geophys. R., 107, A11

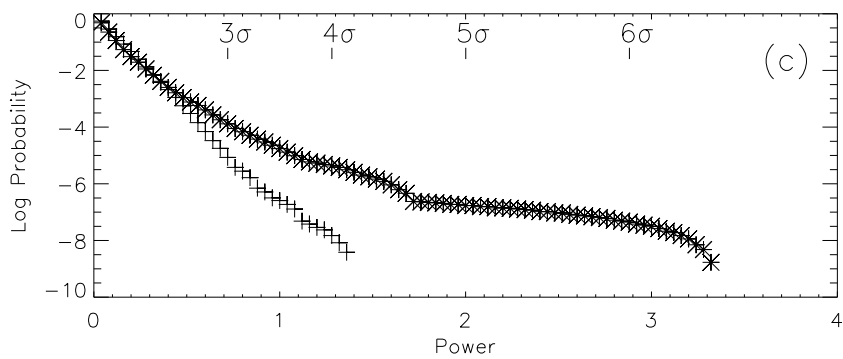
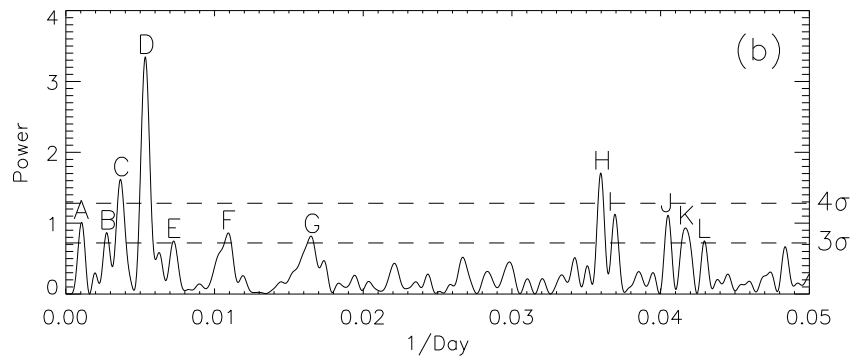
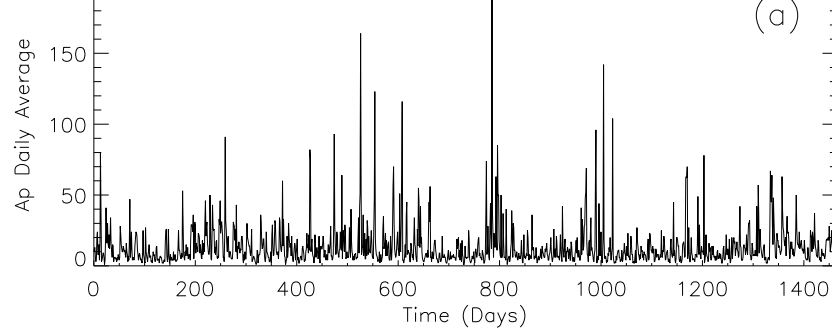
Wolff C. L., 1998, ApJ, 502, 961

Wolff C. L., Blizzard J. B., 1986, Solar Phys., 105, 1

Zirin, H. 1988, *Astrophysics of the Sun* (New York: Cambridge University Press)







This figure "figure4.jpg" is available in "jpg" format from:

<http://arxiv.org/ps/astro-ph/0307277v1>

This figure "figure5.jpg" is available in "jpg" format from:

<http://arxiv.org/ps/astro-ph/0307277v1>

This figure "figure6.jpg" is available in "jpg" format from:

<http://arxiv.org/ps/astro-ph/0307277v1>